

## VARIATIONS IN TOTAL SOLAR AND SPECTRAL IRRADIANCE AS MEASURED BY THE VIRGO EXPERIMENT ON SOHO

Judit Pap,<sup>1</sup> Martin Anklin,<sup>2</sup> Claus Fröhlich,<sup>2</sup> Christoph Wehrli,<sup>2</sup> Ferenc Varadi,<sup>1</sup> and Linton Floyd<sup>3</sup>

<sup>1</sup>University of California, Los Angeles, 405 Hilgard Ave., Los Angeles, CA 90095-1562, USA

<sup>2</sup>Physikalisch-Meteorologisches Observatorium, Davos, 33 Dorfstrasse, CH-7260, Davos-Dorf, Switzerland

<sup>3</sup>Interferometrics, Inc., Chantilly, VA 20151, USA

### ABSTRACT

The Variability Irradiance Gravity Oscillation (VIRGO) experiment on SOHO has been observing total solar and spectral irradiances at 402 nm (blue channel), 500 nm (green channel), and 862 nm (red channel) since January 1996. The VIRGO observations have shown that solar active regions influence both total and spectral irradiances in a similar fashion, although the amplitude of the variations seems to be the largest for the near-UV and visible wavelengths. Comparison of the VIRGO total solar irradiance and the UARS/SUSIM Mg II h & k core-to-wing ratio shows that total irradiance started to rise in prior to UV irradiance, as represented by the Mg core-to-wing ratio. In this paper we review the most recent results on the VIRGO irradiance variations related to solar activity. We dedicate this paper to the memory of Dr. Guenther Brueckner, the late Principal Investigator of the UARS/SUSIM experiment, who will always remain in the heart and memory of the authors of this paper.

### INTRODUCTION

Since the Sun is the fundamental source of energy that sustains life on Earth, the accurate knowledge of the solar radiation received by the Earth and understanding of its variability are critical for environmental science and climate studies. In addition to the terrestrial/climate significance of solar irradiance variations, measurements of the solar energy flux and its variability as a function of wavelength throughout the solar spectrum provide important information about the physical processes and structural changes in the solar atmosphere. Space-based observations of solar irradiance integrated over the entire solar spectrum, hence total irradiance, and at various UV wavelengths started about two decades ago. These irradiance observations established conclusively that both total and UV irradiances vary in parallel with the solar activity cycle (e.g. Willson and Hudson, 1988; Rottman, 1988). Although the overall pattern of solar irradiance variations is similar at various wavelengths, being higher during high solar activity conditions, remarkable differences exist between the magnitude and shape of the observed changes. These differences result from the different physical conditions in the solar atmosphere where the irradiances are emitted.

The time scales associated with solar active regions (from days to months) have revealed interesting and distinct variations in total and spectral solar irradiance. The most striking events in the short-term changes of total irradiance are the sunspot-related temporary dips (e.g. Willson *et al.*, 1981), whereas the short-term variations of UV irradiance are mainly dominated by the effect of plages as they evolve and move across the solar disk (e.g. Donnelly *et al.*, 1983). While considerable information exists about the variations in total solar and UV irradiances, variations in the visible and infrared part of the spectrum are less understood,

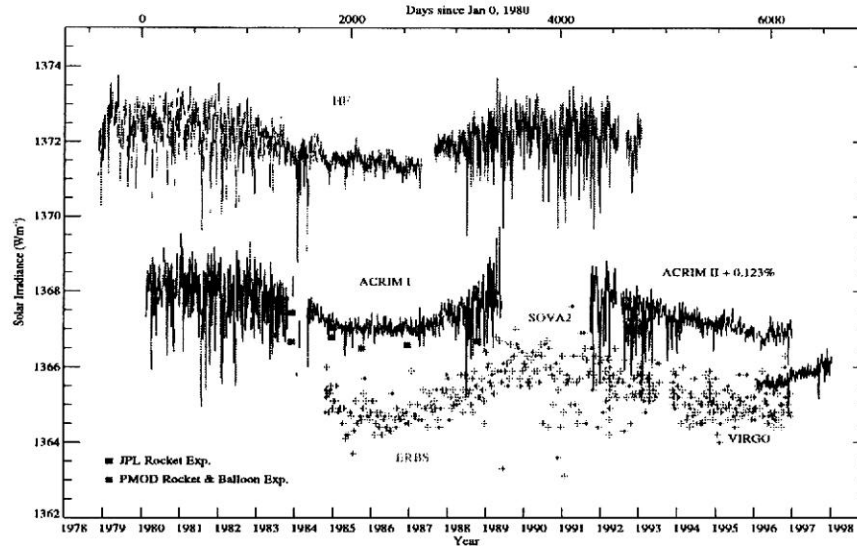


Figure 1: Time series of various space-borne irradiance experiments from Fröhlich (1998).

mainly because of the lack of long-term space-based measurements. The VIRGO experiment on SOHO has provided the first information about changes in solar irradiance in the visible and near-infrared spectral ranges. The VIRGO experiment consists of two different types of active cavity radiometers, the PMO6-V and DIARAD, for monitoring total irradiance, two three-channel sunphotometers (SPM) for the measurement of spectral irradiance at 402, 500, and 862 nm with a bandwidth of 5 nm, and a low-resolution imager, the “Luminosity Oscillation Imager” (LOI) with 16 pixels for measuring the radiance distribution over the solar disk at 500 nm (Fröhlich *et al.*, 1997). In this paper we compare the variations of total irradiance and near-UV, visible, and near-infrared as observed by VIRGO. The VIRGO irradiance data are also compared to the UARS/SUSIM Mg II h & k core-to-wing ratio (Brueckner *et al.*, 1993; Floyd *et al.*, 1998) and the Photometric Sunspot Index (PSI) (Hudson *et al.*, 1982). Since the Mg core-to-wing ratio (thereafter Mg *c/w*) correlates well with the Ca II plage index (Donnelly *et al.*, 1994), it is used as a reasonably good proxy to describe the effect of faculae on the VIRGO solar total and spectral irradiances. To describe the effect of sunspots on solar irradiance, PSI has been derived from the area, position, and contrast of sunspots (Fröhlich *et al.*, 1994), taking into account the area dependence of the contrast (Steinegger *et al.*, 1990).

#### VARIATIONS IN TOTAL SOLAR AND UV IRRADIANCE

The VIRGO total irradiance data provide an important segment of the long-term total irradiance data base. The first and longest total irradiance observations from space were performed by the Nimbus-7/ERB experiment between November 1978 and January 1993 (Kyle *et al.*, 1994). The ACRIM I total irradiance observations started in February 1980 on board the SMM satellite (Willson and Hudson, 1988) and have been continued by the ACRIM II observations on UARS since October, 1991 (Willson, 1997). An additional long-term total irradiance monitoring has been conducted by the ERBE experiment since 1984 (Lee *et al.*, 1995). The EURECA/SOVA experiments provided additional 10-month long total irradiance observations between August 1992 and May 1993 (Fröhlich, 1994). These total irradiance observations are summarized in Figure 1. The different scale of these measurements is related to the absolute accuracy ( $\pm 0.2$  percent) of the calibration of the individual measurements (Fröhlich, 1998). However, the relative precision and stability of the instruments is much better, which makes it possible to study the relative variations in total irradiance.

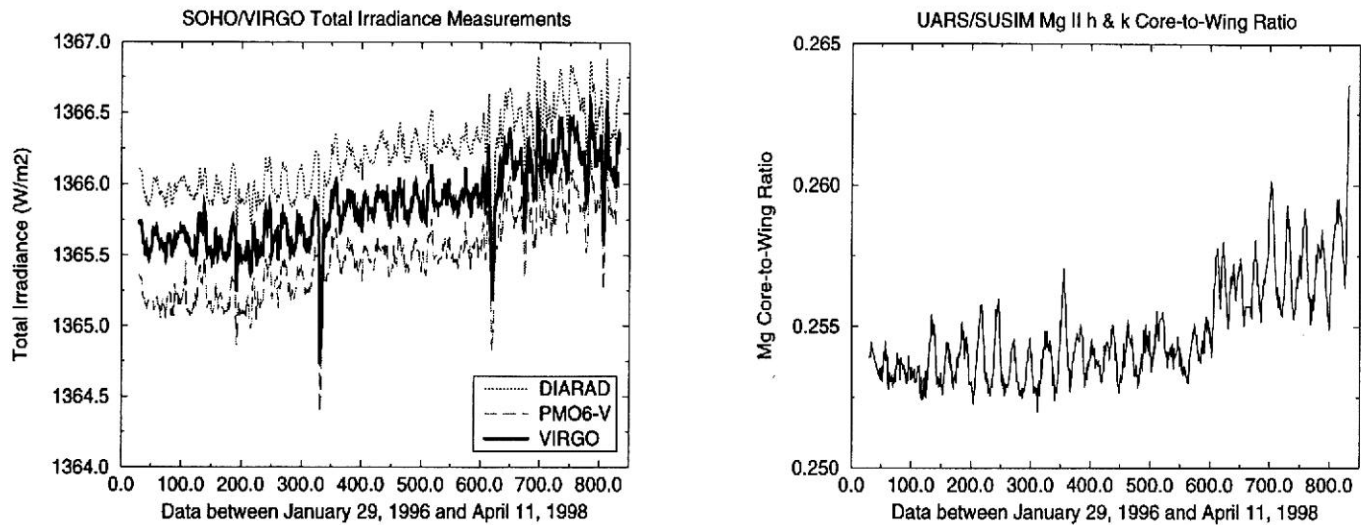


Figure 2: The dotted line of the left-side panel shows the DIARAD total irradiance, the dashed line shows the PMO6-V data. The heavy solid line shows the “VIRGO” total irradiance compiled from the PMO6-V and DIARAD observations. The right-side panel presents the SUSIM Mg c/w ratio (updated from Pap *et al.*, 1998).

The VIRGO total irradiance measurements are presented on the left-side panel of Figure 2 for the time interval of January 29, 1996 to April 11, 1998. The dotted line shows the daily averages of the DIARAD data, the dashed line shows the daily PMO6-V data, whereas the heavy solid line presents the VIRGO total irradiance which is the most accurate composite retrieved from both DIARAD and PMO6-V. Note that both the DIARAD and PMO6-V radiometers are operated in an active mode with a 3-minute sampling cadence for DIARAD and 1-minute for PMO6-V. The “VIRGO total irradiance” data set is compiled from the PMO6-V and DIARAD observations. Since DIARAD exhibits only small changes in its sensitivity, the long-term variability of the VIRGO total irradiance is mainly reflected by the DIARAD measurements (Anklin *et al.*, 1998a). The right-side panel shows the daily values of the V19r3 version of the SUSIM Mg c/w (see details by Floyd *et al.*, 1998). As shown in Figure 2, the effect of active regions is seen in both total irradiance and the Mg c/w. Noting that VIRGO day number 1 corresponds to January 1, 1996, the most remarkable events in the VIRGO total irradiance are the sunspot-related dips around day numbers 330 (November 1996) and 610 (August 1997). During the following solar rotations, especially in the case of the irradiance dip in November 1996, there are substantial enhancements in both total irradiance and the Mg c/w ratio which are due to the increased facular emission. While the faculae-related temporary enhancements in total irradiance and the Mg c/w ratio correlate well, remarkable differences exist between their long-term trends. The VIRGO total irradiance shows a primary rise between December 1996 and May 1997, thereafter, its mean value remains almost constant, and a secondary rise starts after day number 600 (August 1997). By contrast, the SUSIM Mg c/w data remain on a constant level, showing only the effect of solar active regions until August 1997, when a rapid rise started with the increasing activity of the new cycle.

#### VARIATIONS IN THE SOHO/VIRGO SPECTRAL IRRADIANCE

While the VIRGO total irradiance measurements reveal the irradiance changes due to the modulation by active regions and the solar cycle, the evaluation of the VIRGO spectral data is far more difficult, especially because of the degradation of the SPM instrument. The sensitivity of the main instrument has slowly degraded with rates about -52 ppm/day for the 862 nm channel, -310 ppm/day for the 500 nm channel,

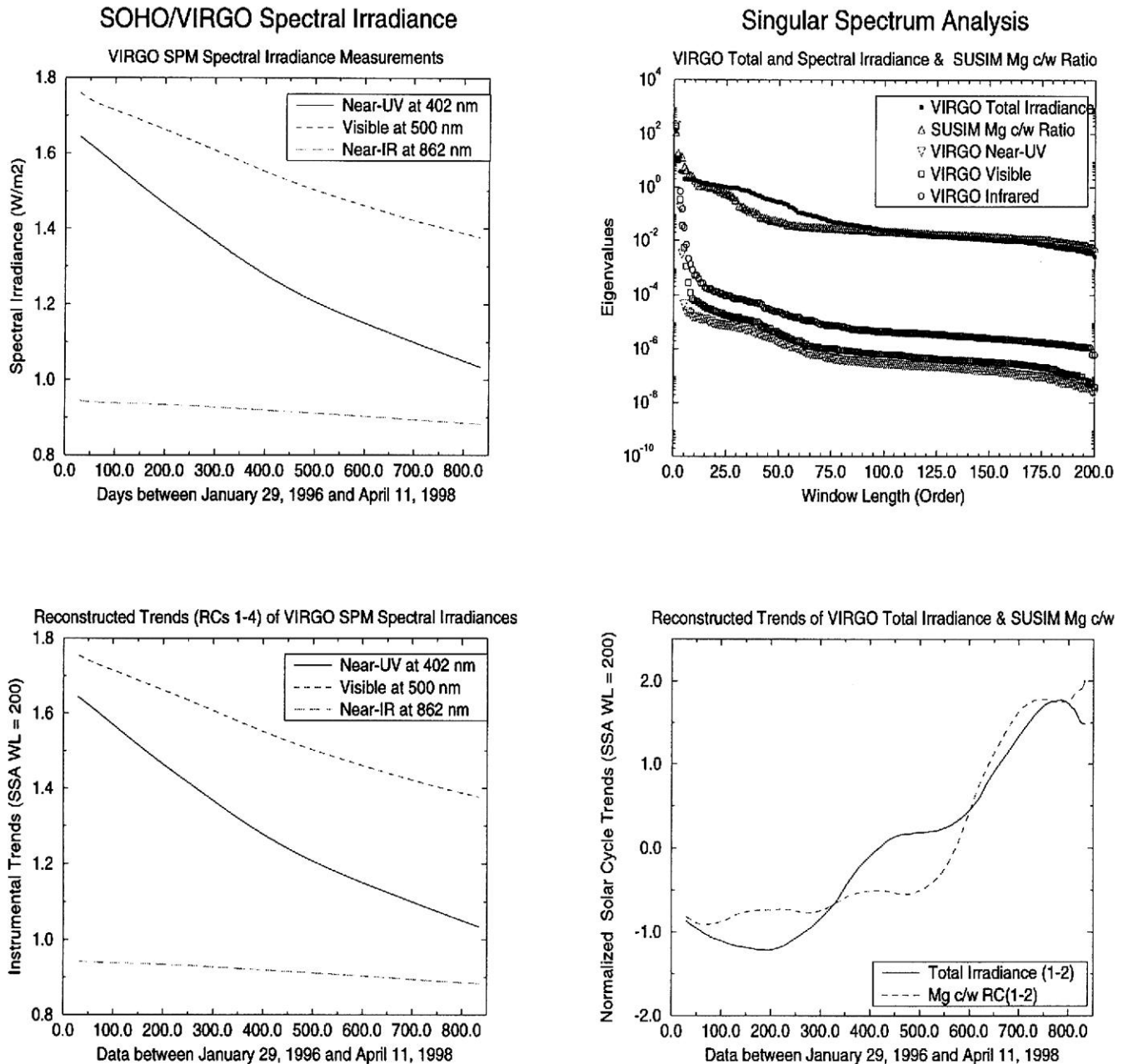


Figure 3: The solid line on the upper left-side panel shows the VIRGO spectral irradiance at 402 nm, the dashed line shows the visible irradiance at 500 nm, and the long-dashed line shows the near-infrared at 862 nm. On the upper right-side panel, the dots show the Singular Spectrum of the VIRGO total irradiance, the triangles up show that of the SUSIM Mg c/w. The triangles down give the spectrum of the VIRGO near-UV, the squares the spectrum of the visible, and the circles give the spectrum of the near-infrared irradiance. The solid line on the left-side of the lower panel represents the SSA-reconstructed instrumental trend for the near-UV, the dashed line shows it for the visible, and the long-dashed line shows it for the near-infrared irradiance. The solid line on the right-side of the lower panel gives the reconstructed solar cycle trend in the VIRGO total irradiance, the dashed line shows the same for the Mg c/w.

and -650 ppm/day for the 402 nm channel (Fröhlich *et al.*, 1997). The observed SPM data are shown on the upper left-side panel of Figure 3. This plot shows that the instrument degradation masks all the solar variability, and the degradation is the largest for the near-UV at 402 nm and the lowest for the infrared. To remove the instrumental trends, we have used a relatively new method, “Singular Spectrum Analysis” (SSA), which was originally developed to study and understand nonlinear and chaotic dynamical systems (Vautard *et al.*, 1992). SSA has been proven as an effective and efficient way to separate unwanted “noise” and “trends” (either solar or instrumental) from the examined signals. Its utility in the study of the noise characteristics of irradiance time series as well as in their decomposition into major oscillatory components was demonstrated by Pap and Varadi (1996), Pap (1997), and Pap and Fröhlich (1998). The cornerstone of SSA is the eigenvalue-eigenvector decomposition of the lag-covariance matrix which is composed of the covariances between a certain number ( $M$ ) of shifted time series, where  $M$  is the so-called “window length”. The eigenvectors of this matrix provide moving average filters which extract uncorrelated parts of the signal and whose contributions to the complete signal are given by the corresponding eigenvalues. The latter are arranged in decreasing order and form the Singular Spectrum.

The Singular Spectra of the VIRGO total and spectral irradiances as well as the SUSIM Mg c/w are presented on the upper right-side panel of Figure 3. As can be seen, the Singular Spectra in each case level off after a certain eigenvalue index and form the so-called “noise-floor”. The number of eigenvalues above the noise floor represents the degree of freedom of the variability and they are associated with the number of oscillatory components in the signal. In most cases, the highest eigenvalues of the Singular Spectra represent the trends in the data – either related to the solar cycle or to instrumental degradation effects. The number of the resolved components, which represent various oscillations in the data, are determined by the window length  $M$ . To avoid statistical errors, the window length should be less than one third of the length of the examined time series (Vautard *et al.*, 1992). In our case, within the above limit for  $M$ , the window length has been chosen as 200. This relatively large window length allows a better separation of oscillatory components, especially trends and low-frequency oscillations. It is interesting to note that the SPM spectral data have much lower noise level than either the VIRGO total irradiance or the Mg c/w – despite the fact that the solar signal is hidden within the instrumental trends.

The most interesting aspect of SSA is the reconstruction of the data above the noise level or part of interest. The various components of the time series can be reconstructed as projection to the appropriate eigenvectors. These “Reconstructed Components” (RCs) are associated with particular oscillations belonging to a subset of eigenvalues. In the case of the VIRGO total irradiance and the Mg c/w, the first two eigenvalues represent the long-term solar-cycle-related trends, these reconstructed trend components are shown on the right-side of the lower panel of Figure 3. As can be seen, both time series show the rise during the ascending phase of solar cycle 23, and this plot demonstrates well the differences between the shape of the two trends. While the VIRGO total irradiance and the Mg c/w correlate with only  $r = -0.02$ , the correlation coefficient is  $r = 0.93$  between the trends. In the case of the SPM data, the instrument degradation trends are related to the first four eigenvalues for each channel (see further details by Pap *et al.*, 1998). The reconstruction of these first four components (RC1-4) for the near-UV, visible, and infrared spectral irradiances is presented on the left-side of the lower panel of Figure 3. As demonstrated, these RCs highly correlate with the measured signals ( $r = 0.9999$ ), in which the most dominating features are the instrumental trends.

The detrended VIRGO total irradiance and Mg c/w, or with other words, their reconstruction without their first two components, are shown on the upper panel of Figure 4; PSI is presented on the lower panel. As this plot shows, the temporary dips in the VIRGO total irradiance correspond to the peaks in PSI, whereas peaks in the detrended VIRGO total irradiance and Mg c/w correspond to each other. Note that at the time of the sunspot-related dips in total irradiance there is usually a small increase in the Mg c/w ratio, which is due to the enhanced faculae radiation in the active regions. The reconstructed SPM data, omitting the first four trend components, are shown on the left-side panel of Figure 5. This plot demonstrates how well SSA removes the dominating instrumental trends, and reveals signals of active regions in the VIRGO spectral irradiances. Unfortunately, the solar-cycle-related trend is also removed this way from the data which may

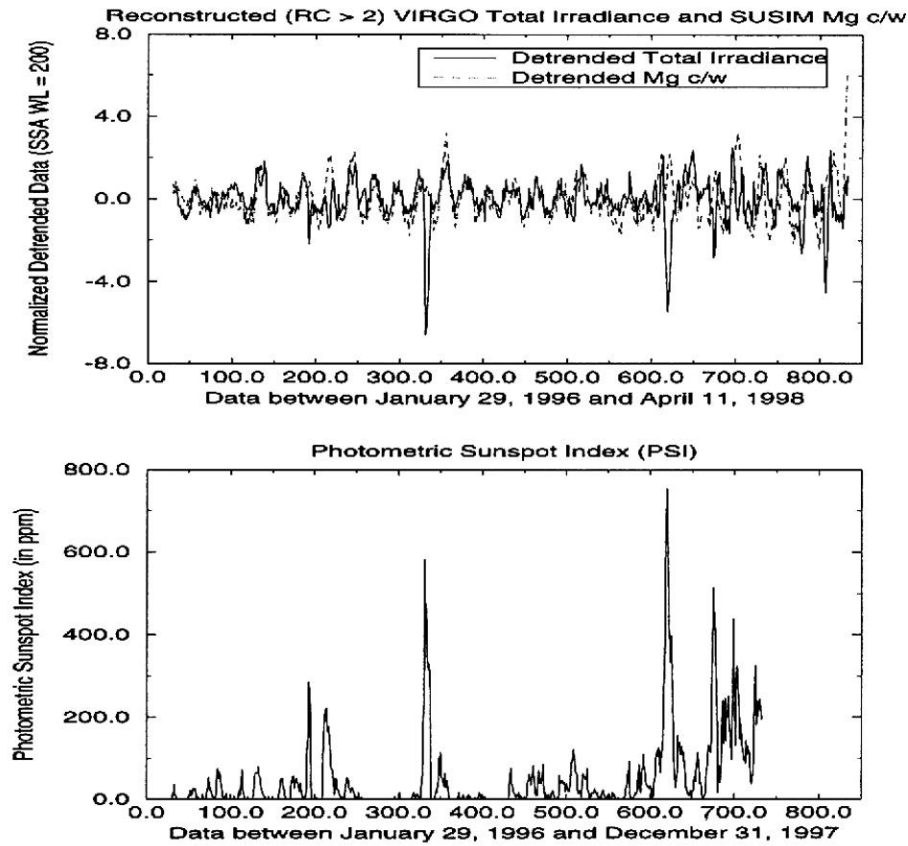


Figure 4: The solid line on the upper panel shows the reconstructed total irradiance omitting the solar-cycle-related two trend components, the dashed line shows the same for the Mg c/w. On the lower panel is given the Photometric Sunspot Index (updated from Pap *et al.*, 1998).

allow us to study only the effect of active regions on spectral irradiance. As an example, the VIRGO near-UV irradiance (solid line) is plotted on the right-side of Figure 5, together with PSI (dashed line) and the Mg c/w (dot-dashed line) to demonstrate the correlation between the VIRGO spectral irradiance variations due to sunspots and faculae. Since the solar-cycle trend is removed from the SPM data, we have plotted the detrended Mg c/w ratio as well. As can be seen, sunspots cause temporary decreases in the VIRGO spectral irradiances, similar to total irradiance, while the temporary enhancements are related to the effect of faculae. It is interesting to note that the amplitude of the variations is usually much higher in near-UV and visible than in the infrared and total irradiance (Wehrli *et al.*, 1998).

## SPECTRAL DISTRIBUTION OF TOTAL IRRADIANCE VARIATIONS

Study of the wavelength dependence of total solar irradiance variations is an important issue since it provides strong and independent constraints on the physical causes of irradiance changes. This is because the radiation at different wavelengths arises in different layers of the solar atmosphere. The various possible driving mechanisms of the irradiance variations are expected to produce temperature changes with different height dependences and hence different wavelength dependences (Solanki and Unruh, 1998). Therefore, knowledge of the spectral distribution of total irradiance variations will also yield a better understanding of the structural changes in the solar atmosphere. Results of Fourier analyses of the VIRGO irradiance data show that between two minutes and 50 days ( $0.23 - 8,300 \mu\text{Hz}$ ) both total and spectral irradiances vary in a similar fashion (Fröhlich *et al.*, 1997; Anklin *et al.*, 1998b). The power spectra of the VIRGO total and spectral irradiances are shown in Figure 6. The highest power is in the frequency range less than  $1.0 \mu\text{Hz}$ ,

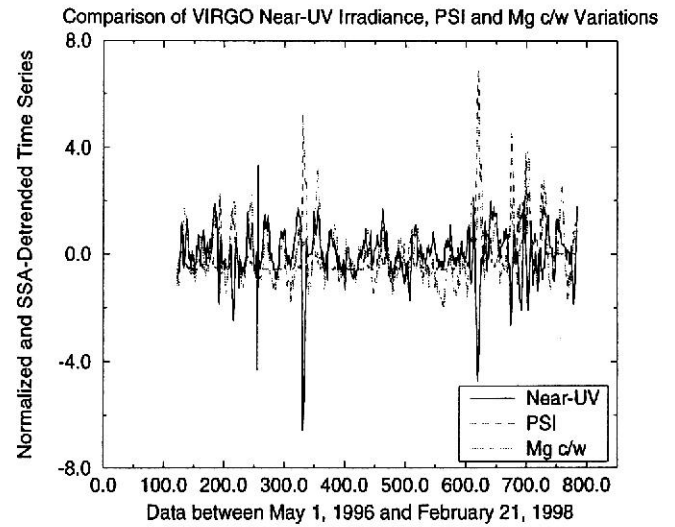
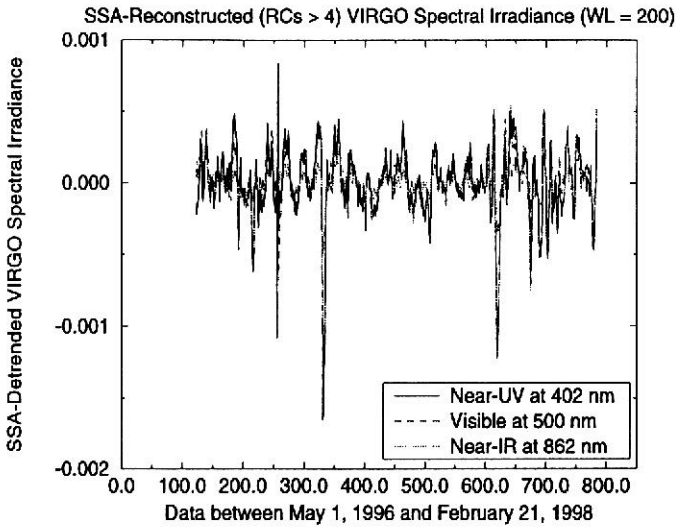


Figure 5: The solid line on the left-side panel shows the near-UV irradiance reconstructed without its first four components (the trend), the dashed line shows the same for the visible and the long-dashed line shows the same for the infrared. The solid line on the right-side panel shows again the “detrended” near-UV data, the dashed line now represents PSI, and the dot-dashed line represents the detrended Mg c/w. The data are plotted for the time interval of May 1, 1996 to February 21, 1998 (updated from Pap *et al.*, 1998).

indicating that active regions cause the strongest modulation in total solar and spectral irradiances. Above  $2.0 \mu\text{Hz}$ , the power declines rapidly. In the  $10 - 100 \mu\text{Hz}$  range the effect of supergranulation is dominant, the meso-granulation covers the  $80 - 1,000 \mu\text{Hz}$ , and the granulation covers the  $800 - 3,000 \mu\text{Hz}$  frequency range. The effect of p-mode oscillations in the  $2,000 - 4,000 \mu\text{Hz}$  is clearly seen in Figure 6. Comparison of the amplitudes of the variations in the three spectral irradiances to that of total irradiance shows that the amplitude of the variations is about 3 to 4 times higher in the near-UV at 402 nm, about 2 to 3 times higher in the visible at 500 nm, and about 1 to 1.5 times higher in the near-infrared at 862 nm than in total irradiance (Fröhlich *et al.*, 1997). Analysis of the nearly two-year long VIRGO data indicates that the ratio of the amplitudes of the variations in total irradiance and the three spectral channels is nearly constant up to  $4,000 \mu\text{Hz}$  (Anklin *et al.*, 1998b).

The contribution of the variations exhibited in the three VIRGO spectral ranges to that of total irradiance has been estimated by means of bivariate and multivariate cross-spectral analyses (see details on these techniques by Fröhlich and Pap, 1989 and Anklin *et al.*, 1998b). As an example, results of the bivariate analysis are presented on the left-side panel of Figure 7 for the near-UV irradiance at 402 nm. The power and cross spectra have been calculated by smoothing the Fourier spectra with a running mean of 31 bins (corresponding to  $0.5 \mu\text{Hz}$ ), and setting the first and last 16 bins to invalid. The upper panel shows the coherence square between total and near-UV irradiances, the corresponding gain and the phase are plotted on the mid and lower panels, respectively. Note that the coherence square gives the degree of linear association between the time series, in this particular case it measures the power at a given frequency of total irradiance which is explained by the variations in the near-UV irradiance at 402 nm. As can be seen, the coherence is high up to  $3.5 \mu\text{Hz}$ , and between  $100$  and  $3,000 \mu\text{Hz}$ . In the lower frequency range the high correlation is related to the fact that both total and near-UV irradiances are modulated by solar active regions in a similar manner, as demonstrated in Figures 4 and 5. In the high frequency range, the high correlation is related to the effect of the convection and p-mode oscillations. As shown in Figure 6, almost all the power of total irradiance in the 5-minute range is explained by the spectral irradiance variations. In contrast, between

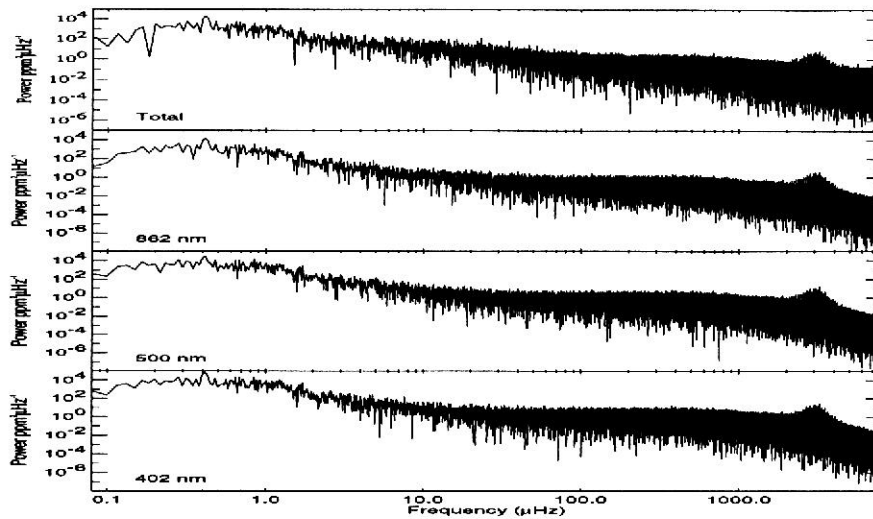


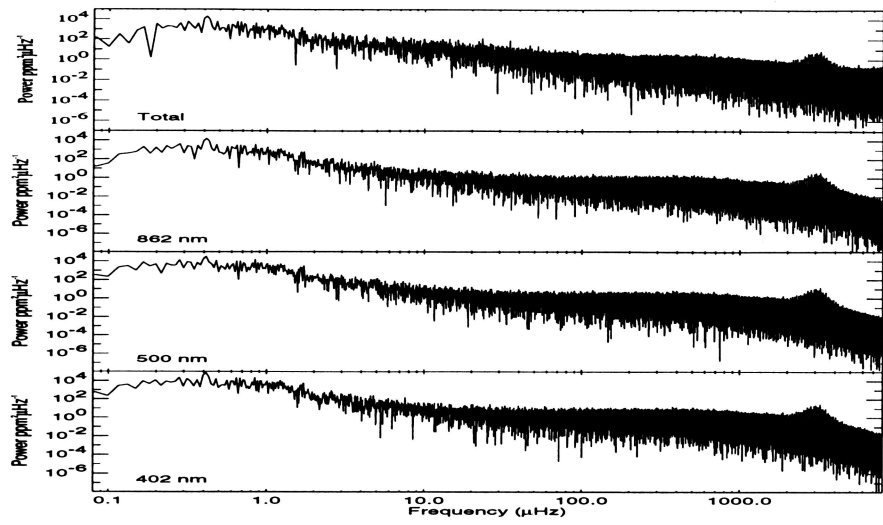
Figure 6: Power spectra of the VIRGO total and spectral irradiances at 862 nm, 500 nm, and 402 nm (updated from Anklin *et al.*, 1998b).

4 and 60  $\mu\text{Hz}$ , the coherence is low for all combinations of the Fourier spectra, and this is attributed to instrumental effects, i.e., differences in the sensitivity and long-term behavior of the instruments (see further details by Anklin *et al.*, 1998b).

Results of multivariate analysis between the VIRGO total irradiance and the three spectral irradiances are presented in the right-side panel of Figure 7 up to 10  $\mu\text{Hz}$ . In this case, the power of total irradiance (shown by the upper curve) is smoothed by 11 bin running means. The shaded areas of the total power indicate the part of the power of total irradiance explained by the variance of the near-infrared, visible, and near-UV irradiances, respectively. The lowest curve shows the residual power of total irradiance which is not explained by the effect of the three spectral irradiances. On average, 75% of total irradiance variations is explained by the variations in the three spectral channels in the frequency range of 0.5 to 3.5  $\mu\text{Hz}$  and note that similar results have been gained for the 200 – 2,000  $\mu\text{Hz}$ . As can be seen, considerable variation remains unexplained in total irradiance, especially between 4 and 10  $\mu\text{Hz}$ , where only 18% of total irradiance variations is explained by the near-UV, visible, and near-infrared spectral irradiances (Anklin *et al.*, 1998b). As mentioned before, this low correlation in the 4 – 10  $\mu\text{Hz}$  frequency range is mainly related to instrumental effects. On the other hand, changes in the UV irradiance below 402 nm may also contribute to the variations in total irradiance. Comparison of the ACRIM I total irradiance and the SME 200 – 300 nm integrated UV irradiance indicated that as much as 50% of total irradiance variations may be explained by the changes in the UV irradiance on the rotational time scale (Pap and Fröhlich, 1992). Recent analysis of Lean (1997), using the UARS/ACRIM II total irradiance and the SUSIM integrated 200 – 400 nm UV irradiance shows that about 30% of the total irradiance variations may be associated with the changes in the integrated UV flux.

## CONCLUSIONS

The VIRGO total solar and spectral irradiance observations have provided important data sets for both solar physics and climate studies. The VIRGO irradiance measurements have shown a wide range of variabilities in both total and spectral irradiances in the near-UV, visible, and near infrared. It has been shown that



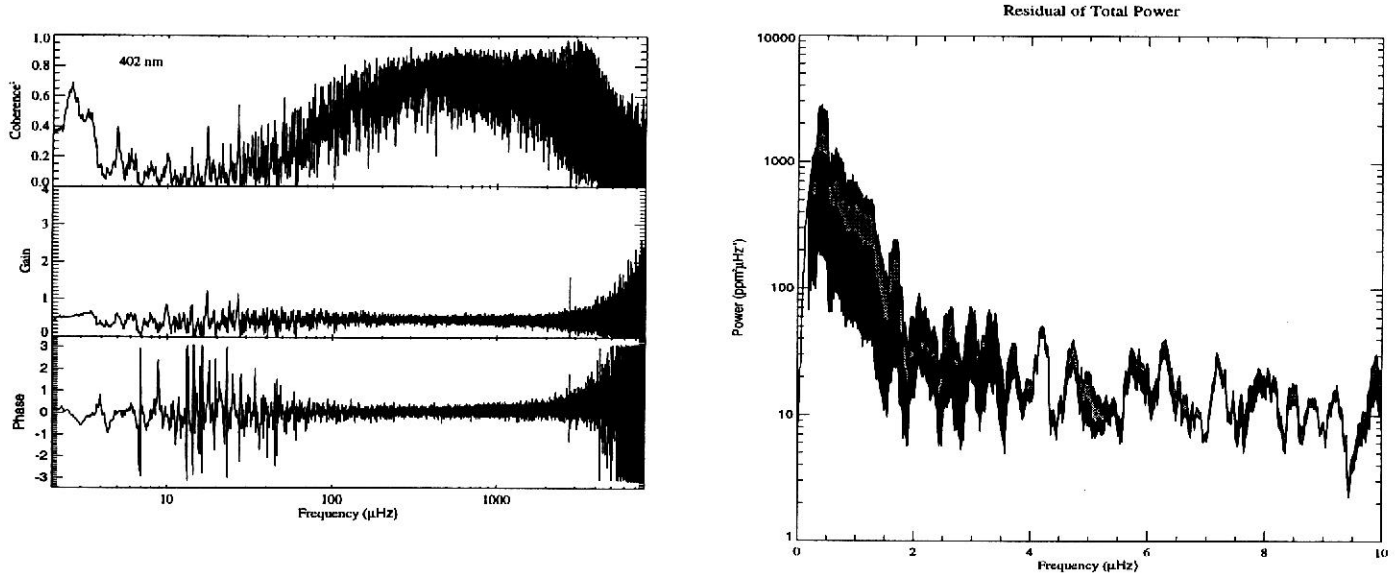
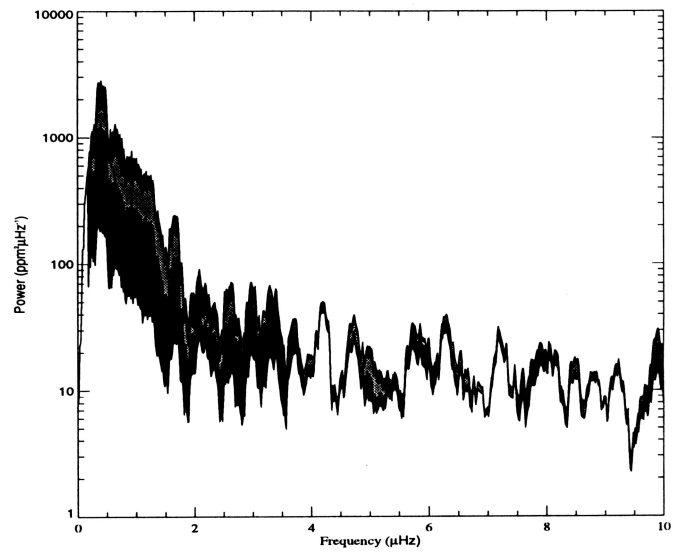


Figure 7: Results of bivariate spectral analysis between the VIRGO total and near-UV irradiances are presented on the left-side panel. The right-side panel shows the results of multivariate analysis between the VIRGO total and three spectral irradiances (updated from Anklin *et al.*, 1998b).

the VIRGO total solar and spectral irradiances vary in a similar fashion in the 0.23 – 8,300  $\mu\text{Hz}$  frequency domain (corresponding to periods of two minutes to 50 days). The power spectra of the VIRGO irradiance data exhibit the prominent p-mode oscillations in the 5-minute range, and it is shown that the spectral variations in this range account for most of the power of total irradiance. The results discussed in this paper show that active regions cause the most prominent variations in both total irradiance and spectral irradiances in the near-UV at 402 nm, visible at 500 nm, and near-infrared at 862 nm via the combined effect of dark sunspots and bright faculae. Comparison of the amplitude of the variations in the almost two-year long VIRGO total irradiance and the three spectral irradiances indicates that the amplitude of the changes is the largest in the near-UV and visible, whereas the changes in the infrared are about the same magnitude as in total irradiance. Results of multivariate analysis indicate that, on average, about 75% of the VIRGO total irradiance variations is explained by the changes observed in the three VIRGO spectral channels, except for the 4 – 20  $\mu\text{Hz}$  frequency domain. In this frequency range only about 18% of the total irradiance variations are related to that of spectral irradiance, and this is mainly due to instrumental effects.

The results discussed in this paper demonstrate the usefulness of SSA in removing instrumental trends which have masked the solar signals in the SPM data. However, the longer-term variations related to the solar cycle have also been removed from the three VIRGO spectral irradiances together with the instrumental trends, therefore we have no information about the variations of the spectral irradiances related to the rising activity of solar cycle 23. Our results indicate that both total irradiance and the UARS/SUSIM Mg c/w ratio started to rise in connection with the ascending phase of solar cycle 23. However, there are remarkable differences between the long-term trends in the total and UV irradiances. Namely, comparison of the VIRGO total irradiance and the SUSIM Mg c/w ratio indicates that total irradiance started to rise several months earlier than the Mg c/w ratio at the beginning of the ascending phase of solar cycle 23. Further studies on this topic are required and they will lead to a better understanding on the underlying mechanisms of irradiance changes.

Residual of Total Power



## ACKNOWLEDGMENTS

The authors gratefully acknowledge the past and ongoing effort of the VIRGO and MDI teams to produce and interpret the SOHO/VIRGO total irradiance data and MDI images. SOHO is a mission of international cooperation between ESA and NASA. This research was funded by a grant NAG53244 from the SOHO Office of NASA's Office of Space Science.

## REFERENCES

- Anklin, M., C. Fröhlich, W. Finsterle, D. Crommelynck, and S. Dewitte, *Metrologia* No 3, in press (1998a).
- Anklin, M., C. Fröhlich, Ch. Wehrli, and W. Finsterle, In *Structure and Dynamics of the Interior of the Sun and Sun-Like Stars*, edited by S.G. Korzennik and A. Wilson, ESA-SP 418, in press (1998b).
- Brueckner, G.E., K.L. Edlow, L.E. Floyd, J. Lean, and M.E. Van Hoosier, *J. Geophys. Res.*, **98**, 10,695 (1993).
- Donnelly, R.F., D.F. Heath, J. Lean, and G.J. Rottman, *J. Geophys. Res.*, **88**, 9883 (1983).
- Donnelly, R.F., O.R. White, W.C. Livingston, *Solar Physics*, **152**, 69 (1994)
- Floyd, L.E., L.C. Herring, P.C. Crane, D.K. Prinz, and G.E. Brueckner, G.E., *Adv. Space Res.*, in press (1998).
- Fröhlich, C. and J. Pap, *Astron. Astrophys.*, **220**, 272 (1989).
- Fröhlich, C., J. Pap, and H.S. Hudson, *Solar Physics*, **152**, 111 (1994).
- Fröhlich C., In *The Sun as a Variable Star: Solar and Stellar Irradiance Variations*, edited by J.M. Pap, C. Fröhlich, H.S. Hudson, S.K. Solanki, Cambridge Univ. Press, pp. 28 (1994).
- Fröhlich C., In *Solar Electromagnetic Radiation Study fo Solar Cycle 22*, edited by J.M. Pap, C. Fröhlich, R. Ulrich, Kluwer Academic Publishers, pp. 391 (1998).
- Fröhlich et al., *Solar Physics*, **170**, 1 (1997).
- Hudson, H.S., S. Silva, M. Woodard, and R.C. Willson, *Solar Physics*, **76**, 211 (1982)
- Kyle, H.L., D.V. Hoyt, and J.R. Hickey, *Solar Physics*, **152**, 9 (1994).
- Lean, J., *J. Geophys. Res.*, **D25**, 29,939 (1997)
- Lee R.B., M.A. Gibson, R.S. Wilson, and S. Thomas, *J. Geophys. Res.*, **100**, 1667 (1995).
- Pap, J., and C. Fröhlich, In *Proceedings of Solar Electromagnetic Radiation Study for Solar Cycle 22*, edited by R.F. Donnelly, NOAA/ERL/SEL, pp. 62 (1992).
- Pap, J., and F. Varadi, In *Solar Drivers of Interplanetary and Terrestrial Disturbances*, edited by K.S. Balasubramaniam, S.L. Keil, and R.N. Smart, P.A.S.P. 95, pp. 576 (1996).
- Pap, J., In *Past and Present Variability of the Solar-Terrestrial System: Measurement, Data Analysis and Theoretical Models*, edited by G.C. Castagnoli, A. Provenzale, Italian Physical Society, IOS Press, Amsterdam, pp. 1 (1997).
- Pap, J., C. Fröhlich, M. Anklin, Ch. Wehrli, F. Varadi, and L. Floyd, In *Structure and Dynamics of the Interior of the Sun and Sun-Like Stars*, edited by S.G. Korzennik and A. Wilson, ESA-SP 418, in press (1998).
- Pap, J., and C. Fröhlich, *J. Atmospheric and Solar Terr. Phys.*, in press (1998).
- Rottman G.J., *Adv. Space Res.*, Vol. **8**., No. 7, pp. 53 (1988)
- Solanki S.K., and Y. Unruh, *Astron. Astroph.* **329**, 747 (1998).
- Steinegger, M., P. Brandt, J. Pap, and W. Schmidt, W., *Astrophys. Space Sci.*, **170**, 127 (1990).
- Vautard, R., P. Yiou, and M. Ghil, *Physica D*, Vol. **35**., 395 (1992).
- Wehrli, Ch., T. Appourchaux, D. Crommelynck, W. Finsterle, and J. Pap, In *Sounding Solar and Stellar Interiors*, edited by J. Provost, F.-X. Schmider, Kluwer Academic Publishers, pp. 209 (1998).
- Willson, R.C., S. Gulkis, M. Janssen, H.S. Hudson, and G.A. Chapman, *Science*, **211**, 1114 (1981).
- Willson, R.C., and H.S. Hudson, *Nature*, **332**, 810 (1988)
- Willson R.C., *Science*, **277**, 1963 (1997).